ERDC/CERL TR-06-2

US Army Corps of Engineers®
Engineer Research and Development Center

Techniques To Remotely Identify and Evaluate Electrical Power System Infrastructure

Tarek Abdallah, Michael K. McInerney, William R. Taylor, and Carl A. Feickert

February 2006

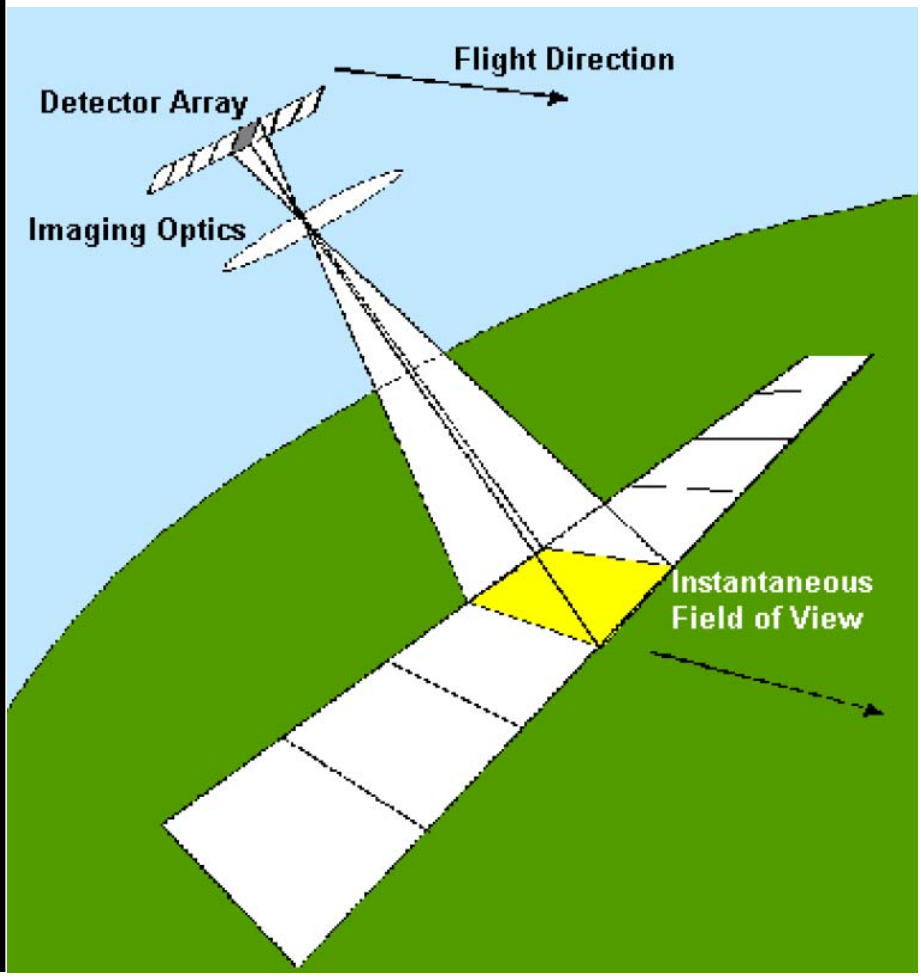

Construction Engineering Research Laboratory

ERDC/CERL TR-06-2
February 2006

Techniques To Remotely Identify and Evaluate Electrical Power System Infrastructure

Tarek Abdallah, Michael K. McInerney, William R. Taylor, and Carl A. Feickert

Construction Engineering Research Laboratory
PO Box 9005
Champaign, IL 61826-9005

Final Report

Prepared for U.S. Army Corps of Engineers
Washington, DC 20314-1000

Under Work Unit 8H08FB

ABSTRACT: It can be difficult for military planners to assess potential sites when establishing forward facilities for deployed military units in austere environments. They must consider many parameters; e.g., geographic elevation and contiguous flat terrain, proximity to operating electrical distribution systems, etc. Since potential site locations may be in hostile territory, remote detection and assessment of electrical systems can be essential. Because such systems emit signals and/or have passive signatures, a potential source of identification can be examined when viewed from above the earth or from a distance when on the ground. This work reviews the basic signal and signatures of electrical systems and identifies parameters most pertinent to their remote detection.

Contents

List of Figures and Tables

Figures

Tables

Conversion Factors

Non-SI* units of measurement used in this report can be converted to SI units as follows:

Multiply	By	To Obtain
acres	4,046.873	square meters
cubic feet	0.02831685	cubic meters
cubic inches	0.00001638706	cubic meters
degrees (angle)	0.01745329	radians
degrees Fahrenheit	(5/9) x (°F – 32)	degrees Celsius
degrees Fahrenheit	(5/9) x (°F – 32) + 273.15.	kelvins
feet	0.3048	meters
gallons (U.S. liquid)	0.003785412	cubic meters
horsepower (550 ft-lb force per second)	745.6999	watts
inches	0.0254	meters
kips per square foot	47.88026	kilopascals
kips per square inch	6.894757	megapascals
miles (U.S. statute)	1.609347	kilometers
pounds (force)	4.448222	newtons
pounds (force) per square inch	0.006894757	megapascals
pounds (mass)	0.4535924	kilograms
square feet	0.09290304	square meters
square miles	2,589,998	square meters
tons (force)	8,896.443	newtons
tons (2,000 pounds, mass)	907.1847	kilograms
yards	0.9144	meters

*_Système International d'Unités_ ("International System of Measurement"), commonly known as the "metric system."

Preface

This study was conducted for Headquarters, U.S. Army Corps of Engineers (HQUSACE) under Project 4A162784AT41, "Military Facilities Engineering Technology"; Work Unit 8H08FB, "Power System Remote Assessment Work." The Technical Monitor was Dr. Paul A. Howdyshell, CEERD-CV-ZT.

The work was performed by the Energy Branch (CF-E), and the Materials and Structures Branch (CF-M) of the Facilities Division (CF), and the Construction Engineering Research Laboratory (CERL). The CERL Principal Investigators were Tarek Abdallah and Michael K. McInerney. Dr. Thomas Hartranft is Chief, CEERD-CF-E, Martin J. Savoie is Chief-CF-M, and L. Michael Golish is Chief, CEERD-CF. The associated Program Manager was Mr. Kirk McGraw and the Technical Director was Dr. Paul A. Howdyshell, CV-ZT. The technical editor was William J. Wolfe, Information Technology Laboratory. The Acting Director of CERL is Dr. Ilker R. Adiguzel.

CERL is an element of the U.S. Army Engineer Research and Development Center (ERDC), U.S. Army Corps of Engineers. The Commander and Executive Director of ERDC is COL James R. Rowan, and the Director of ERDC is Dr. James R. Houston.

1 Introduction

Background

Military planners who assess potential sites for forward facilities to accommodate deployed military units in austere environments must consider a number of logistical factors, e.g., geographic elevation, or the amount of contiguous flat terrain. Another potentially useful factor is the site's proximity to operating electrical distribution systems (Figure 1). Assessing a site's proximity to an operating electrical distribution system can be considered an additional input factor in solving a "region aggregation problem" (Wallace 2003).

However, since such potential sites may be in hostile territory, there would be a great logistical advantage in performing the site evaluation (and detecting electrical systems) remotely. This is possible because the operation of electrical systems characteristically creates electro-magnetic (EM) and acoustic emissions. These electrical or acoustic signatures may potentially identify the system from a distance, either viewed from above the earth or detected from a distant ground location.

The Engineer Research and Development Center, Construction Engineering Research Laboratory (ERDC-CERL) is currently developing a software tool to assist military planners in remotely assessing the feasibility of such potential sites. A software tool that would detect and characterize this signal must first consider basic EM and acoustic signatures of electrical systems and identify the parameters most pertinent to remote detection of electrical distribution systems.

Objectives

The objectives of this work were to:

1. Review the basic EM and acoustic signatures of electrical systems
2. Identify the parameters most pertinent to remote detection of electrical distribution systems
3. Identify signals and signatures of greatest interest for use in remote detection.

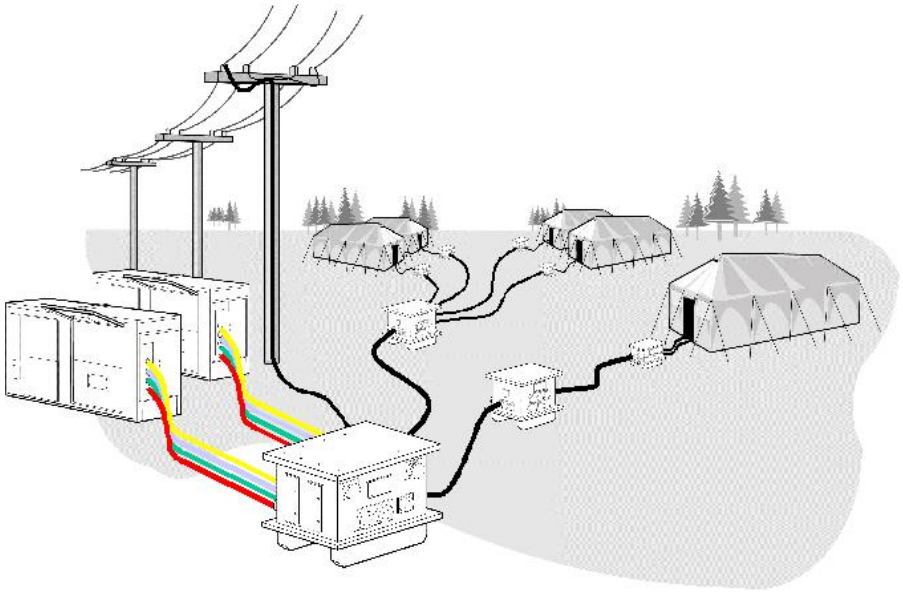

Figure 1. Forward operating bases can be powered by in-theater distribution as well as mobile generation assets.

Approach

1. Basic EM and acoustic signatures of electrical systems are enumerated.
2. A simple explanation of the elementary physics for detection of signals and signatures is provided.
3. A discussion of signature parameters and their limitations/strengths is also provided.
4. Several off-the-shelf hardware products capable of remote detection are presented as an example of present remote detection capabilities.

Scope

This work conducted an initial exploration of electrical signatures with potential for remote detection. With the exception of the hardware products discussed, using other signals or signatures for remote detection would likely require considerable basic research and development prior to being ready for field application.

The information presented here is intended to supply a general understanding of how identification and assessment of electrical power system infrastructure in foreign lands can influence the site selection challenge for forward operating bases. Further, the report provides a technical explanation of a number of discrete technologies and their capabilities and limitations when sensing various components of

electrical power system infrastructure. This information is of great value to military planners as future forward operating base site selection practices will rely on such advanced remote sensing technologies.

Mode of Technology Transfer

Upon publication, this report shall be made accessible to its sponsor as well as to Department of Defense agencies and personnel to which the contents of this report are pertinent. This report and its findings will be published as an ERDC technical report and will be made accessible through the World Wide Web (WWW) at URL:
http://www.cecer.army.mil

2 Overview of Remote Assessment and Power System Operation

Remote assessment can be defined as the:

> collection or measurement of information about a target without being in physical contact with the object (TEC 2005). Aircraft and satellites are the most common platforms used for remote sensing observations. Methods of remote sensing usually employ electromagnetic energy, such as light, heat, and radio waves to detect and measure target characteristics (TEC 2005).

Remotely determining characteristics of objects on the ground usually follows four logical steps:

1. *Data Collection* (e.g., acquiring images, or spatial matrices describing characteristics such as reflectivity of radiation)
2. *Data Analysis*
3. *Image Recognition* (determining whether data in a specific region conform to predefined patterns known to be associated with terrain or infrastructure features)
4. *Object Attribute Identification* (resolving whether specific attributes of infrastructure objects can be inferred such as condition, capacity, or mode of operation).

Characteristics of remote assessment systems include spatial resolution, spectral coverage, and temporal frequency (TEC 2005). Spatial resolution refers to the level of discretization (i.e., how fine a matrix is generated to represent the target region, or how detailed an image). Spectral coverage refers to how large a portion of the EM spectrum is captured. Temporal frequency refers to the frequency of data capture. Since this work assumes that remote assessment will be used to determine the existence and mode of operation of electrical power systems, it must first consider the nature of electrical power system operation. The remainder of this chapter outlines how commercial power is transmitted over long distances and describes the infrastructure used in this process.

Centralized power is generated at power plants and is transmitted over long distances as high voltage alternating current. Alternating current transmission has become standard because rectification to direct current is inexpensive and trivial. High voltages (275 kV-400 kV) are used to reduce line power loss (I^2R) when transmitting large quantities of power. Although many of the largest power transmission

corridors are rated to carry more than 3000 Amperes, most will carry roughly 600-700 Amps during steady-state conditions. Typically, lines have a ground clearance of roughly 8 to 10 meters. The highest field magnitudes directly attributable to line current can be measured on the ground directly below the conductor cables. Typical field measurement values during normal conditions range between 25-150 uT. The field effect geometry that results from these high power transmission corridors exhibits a dependence on conductor arrangement (e.g., steel-reinforced aluminum conductors, steel-supported aluminum conductors), sag coefficients, and line phase ordering protocols. A component of the total field depends on the relative phasing of the energized circuits. Untransposed phasing line arrangements have the phases in the same order descending along the tower on each side. This geometry can be modeled as a single "infinitely long" conductor (Figure 2) with current bounded by a circular closed contour. (It obeys the classical electromagnetic field solution, which decays as the inverse square of distance from the line.) Lines with transposed phasing arrangements have the opposite order of phasing on either side of the tower.

$$\oint_S \overline{B} \cdot d\overline{S} = u_0 I \qquad \text{Eq 1}$$

The sum of enclosed currents bounded by the closed contour defined under Ampere's Law (Eq. 1) indicates an extra cancellation between the fields from the equal but opposing currents on the two sides, and as a consequence, the field decays more approximately as the inverse cube of distance, producing a much lower field at large distances from the line. For example, if a given field point sensor can detect energized untransposed system operation from a monitoring distance of 10 km, the same sensor would need to be closer than 4.64 km to detect the transposed case at the same level of power transmission. (Later in this report, we will find that sensors capable of detecting field strength traces in the microtesla range are required to reliably sense power system EM emissions.)

Power System Signals and Signatures

The available techniques for remote detection of electrical systems include direct field effects and electrical signatures (electric fields, magnetic fields, and corona) as well as various spectral and physical emissions (acoustic, visible, infra-red, and hyper-spectral). Components of an energized electrical distribution system will inherently have associated signals or signatures. Whether these signatures are detectable from any practicable distance beyond the immediate proximity to the component depends on their operating parameters and the physical limitations of the assessment technique.

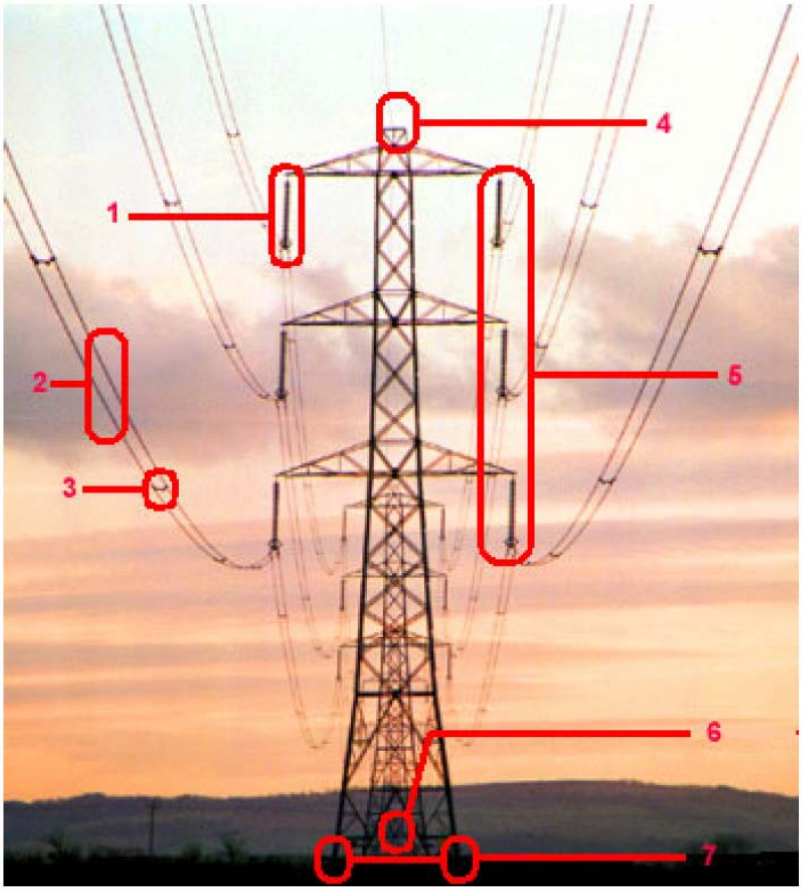

1. Insulator.
2. Bundle of two conductors (some lines have 4).
3. Spacer to hold the two conductors apart.
4. Earth wire at top of tower or pylon.
5. The three bundles on one side of the tower make up one electrical circuit. Most lines have two circuits, one each side.
6. Identity plate saying which line it is and who owns it.
7. Anti-climbing device - barbed wire to stop unauthorised climbing

Figure 2. A typical transmission tower (Energy Network Assn. 2005).

This chapter discusses the basic physics of electrical components' signals or signatures with minimal regard for the practicality of remotely detecting such signals. In addition to remotely detecting the presence and location of electrical systems, a related issue is remote determination of electrical system capacity and loading based on optical recognition and emitted signals or signatures. Therefore, a discussion of the physics of (visually observable) thermal expansion is included as a possible means of remotely assessing system loading.

Transmission lines carry electrical power that flows alternately in one direction and then reverses 50 or 60 times per second. The presence of charges on these conductors and their temporal variations give rise to distinct physical phenomena: electric and magnetic fields.

Electric and Quasi-Static Fields

When electric charges exist in the free state, they exert a mutual force upon each other. At any given spatial point, the ratio of this force magnitude per unit charge, is referred to as the electric field strength, E. This is a vector function and has the convention of pointing away from "+" charges, and towards "–" charges. Charged metallic surfaces, such as electrical power transmission lines, have these charges localized to the physical surface of the conductor. And their presence and physical effects may be sensed in a number of ways, primarily related to the electric field.

Consider a power transmission line that, at any instant of time, is charged to a potential V_o (Volts) relative to the ground, and further to be a long straight conductor of radius, a, and parallel to the ground which is located a distance h, below the line. Then the magnitude of the associated electric field a radial distance, r (meters) from the center of the conductor, can be shown to be (approximately, for r < h/10):

$$E(\text{volts/meter}) = \frac{V_0}{(r \ln(\frac{h}{a}))} \qquad \textbf{Eq 2}$$

Examination of Equation 2 shows that, for a sufficiently large V_o, E may become large enough to cause local ionization of the air at the surface of the conductor. An electric field may be shielded (e.g., reduced in strength) by any conductive or dielectric surface, such as trees, walls, or buildings.

Magnetic Fields

To transmit electrical power, electrical charges must be set in motion by an electrical field. This flow of charge is referred to as electrical current, and usually derives from a battery or electrical generator source. A direct physical consequence of the electrical current is an associated magnetic field, the strength of which is a function of the current flow, but not of the voltage present on the conductor.

Faraday's Law

The simple loop receiving antenna—the most conceptually simple design available—is governed by Faraday's law:

$$\oint_C \overline{E} \cdot d\bar{l} = -\frac{d}{dt}\int_S \overline{B} \cdot d\overline{S} \qquad \text{Eq 3}$$

where:

$\overline{E}$ is the electric field

$\overline{B}$ is the magnetic flux density

Eq 3 is expressed in units of flux.

Since Faraday's law relates the magnetic flux penetrating a surface and the electric potential across the two end points of a line defining that surface, it clearly relates the voltage around one of the coils to the time rate of change of the magnetic flux density through the surface enclosed by that loop (Figure 3). Again consider the transmissions line of Figure 2. If the current flowing in the line is I (Amps), then the associated magnitude of the magnetic field, a radial distance, r (meters) from the center of the conductor can be shown to be:

$$\mathrm{B(Tesla)} = \frac{\mu_0 \mathrm{I}}{2\pi \mathrm{r}} \qquad \text{Eq 4}$$

The constant μ_o, is defined as: $4\pi 10^{-7}$ (Ohm second / meter). The field strengths of B and E have the same (1/r) geometrical dependence relative to the conductor surface.

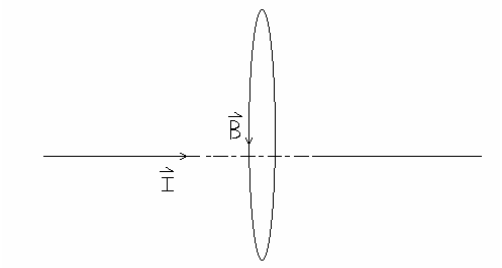

Figure 3. A distribution of current imparts a flux density that obeys the right-hand rule.

Figure 4 shows field measured values of static electric and magnetic fields in the proximity of transmission towers. A typical magnetic field, such as naturally exists near the earth (B ~ 0.0001 Tesla), is quite easily sensed using simple instrumentation such as a compass (constant field) or closed loop of wire connected to a voltmeter (time varying field).

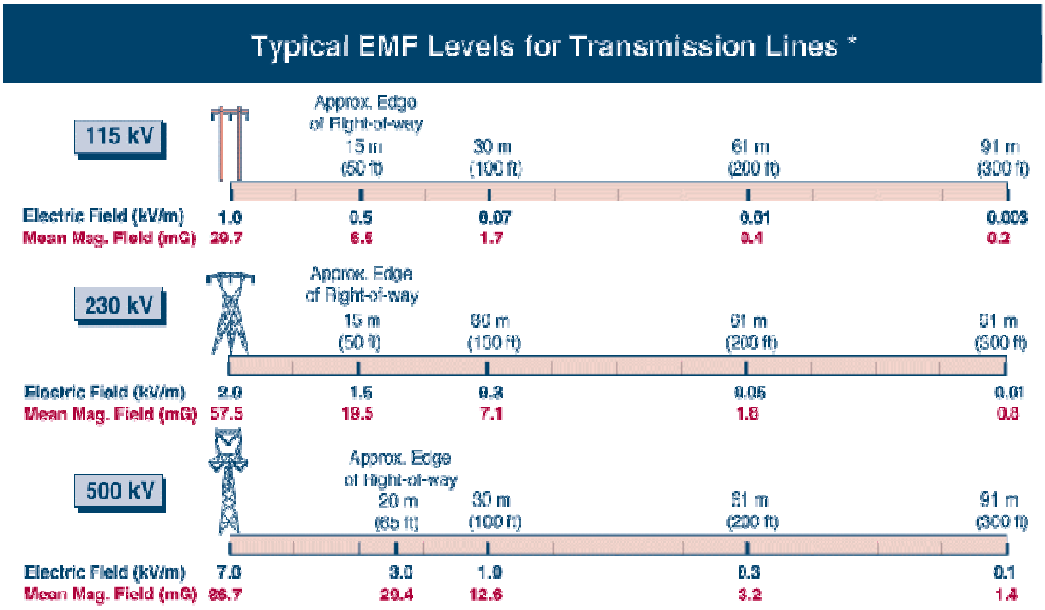

Figure 4. Measured field magnitudes near high-voltage transmission lines (Information Ventures).

For comparison, a field of comparable magnitude (10^{-4} Tesla) is easily generated at a distance of r = 1 meter, from a typical transmission line carrying approximately 500 Amps. Unlike electric fields, most common materials have little shielding effects on magnetic fields (magnetic fields are not easily shielded). This allows these signatures to be detected remotely. Figure 5 shows an area (approximately 12 km by 18 km) surveyed by the GEM-2A remote sensor system (GEOPHEX Engineering 2005). Nominal sensor height was 30 meters above ground level (Won et al. 2003). Chapter 4 of this report reviews several commercial remote assessment systems.

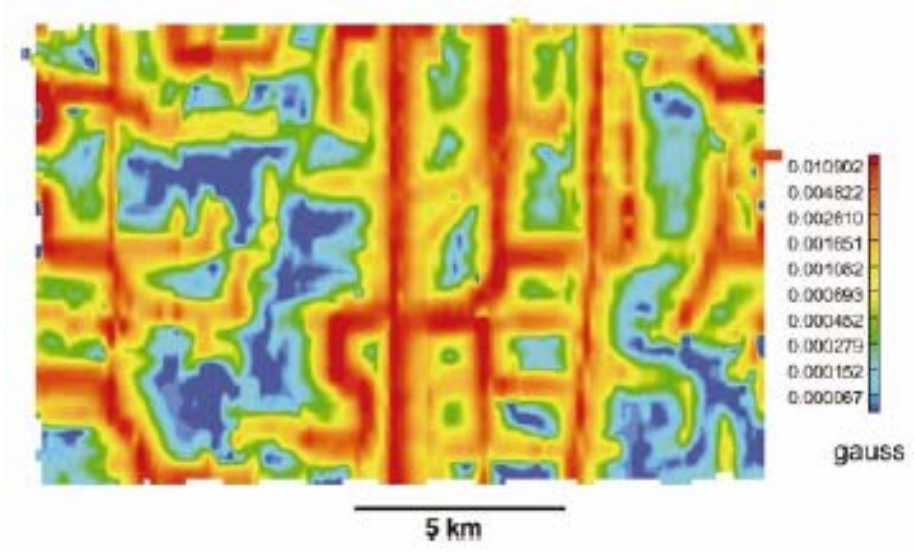

Figure 5. Magnetic field intensities at 60 Hz; high-magnitude linear features can be correlated to power lines (Won et al. 2003).

EM Emissions Near Substations

Detection of electromagnetic emissions near substations is another way to identify the energized state and power level in a given region. In an air-insulated substation (AIS) below an energized bus, the vertical E field and horizontal H field were measured with respect to the bus voltage and field point location (Table 1).

Table 1. Field magnitudes at varying field point locations in a substation switch yard.

h (meter)	Ev (115kV)	Ev (230kV)	Ev (500kV)	Hh(115kV)	Hh(230kV)	Hh(500kV)
h = 0 meter	7 kV/m	5.5 kV/m	13.5 kV/m	36.7 A/m	70.4 A/m	157 A/m
h = 1 meter	14 kV/m	—	—	45.2 A/m	82.2 A/m	—
h = 2.3 meter	15.3 kV/m	—	—	56.1 A/m	—	—
bus height	4.88	5.18	8.33	4.88	5.18	8.33

The first observation from the data in Table 1 is that the "H" field magnitudes show a greater correlation with actual system voltage than the "E" fields. Note that there is an inverse relation between substation voltage and the dominant frequency, as would be expected (Figure 8).

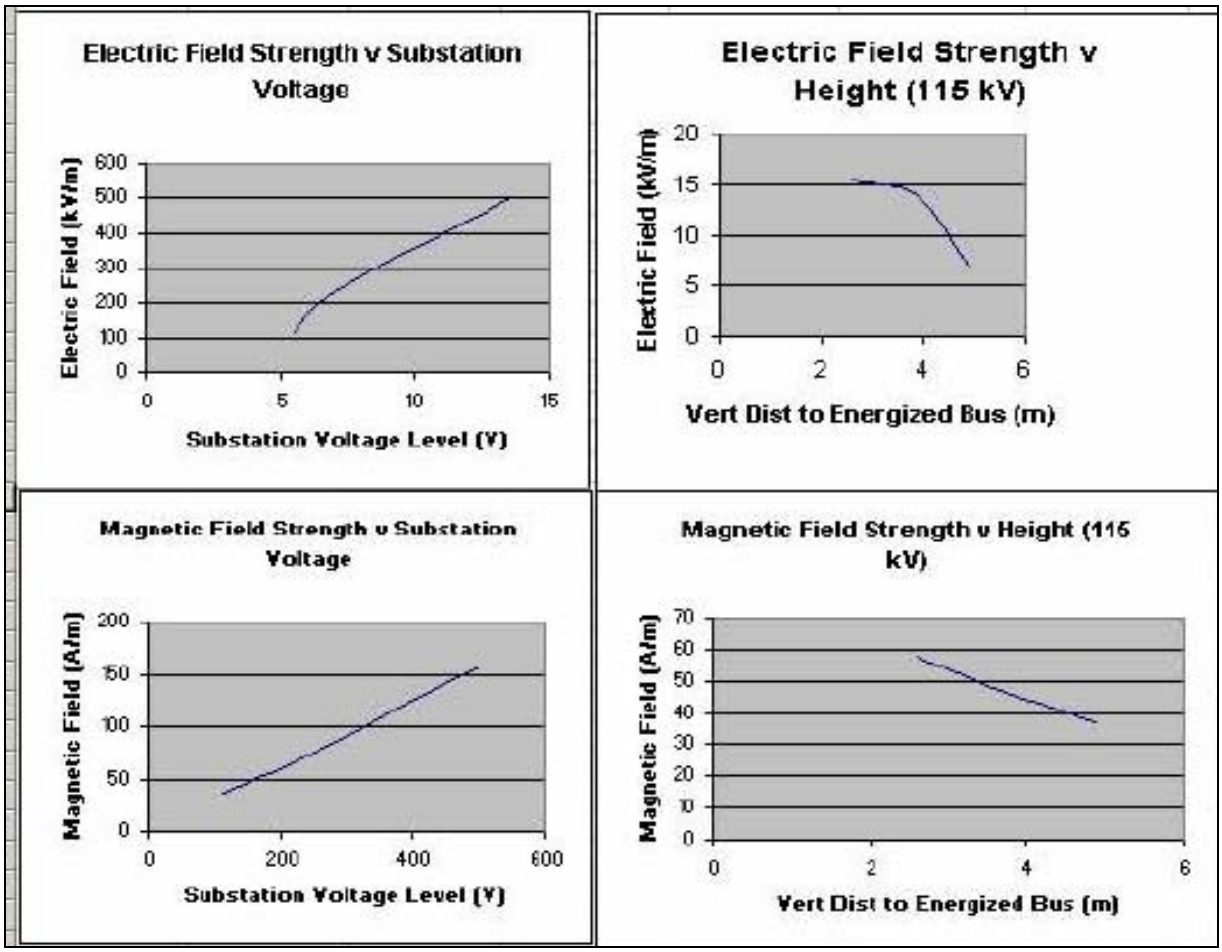

Figure 6. H-Field and E-field strength with bus voltage and distance.

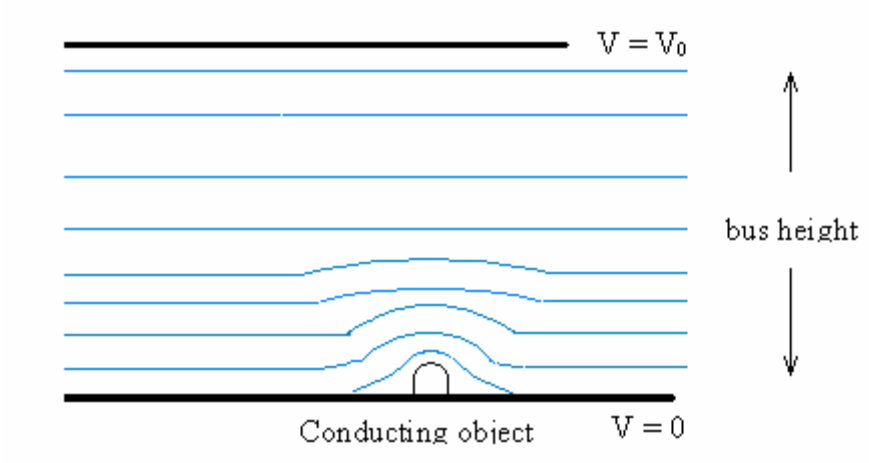

Figure 7. Equipotential lines in the substation switchyard.

Conceptually, the data in Table 1can be explained by elementary electromagnetics. The geometry of the excited bus and ground are considered as two parallel planes of uniform potential that serve as boundary conditions, and the field strength that obeys a "1/r" field decay between them from V_0 to 0 (Figure 7). The geometry of the system becomes more complex when considering effects of metal objects on the ground. Field strength in free space above protruding conducting members in the switchyard is several times greater that would be expected by solution of the simple boundary condition problem. Conceptually, this can be inferred as the tendency of equipotential lines to bend and grow closer to comply with system geometry.

Radio Frequency Interference (RFI)

While a great majority of power systems operate at 60 or 50 hertz, nonlinear loads (e.g., rectifiers, imperfect machines, and motors) can generate high frequency harmonics (multiples of the fundamental frequency) along power lines. As a result, signals with substantial radio frequency components may be carried along transmission lines (and substation equipment) carrying harmonics in the kilohertz range over a wide range of frequencies. A frequent observation made by high-frequency radio operators is that noticeable RF emissions can be correlated to power system components including power factor corrective capacitor banks on power poles. RF-level noise can also be observed near conductors with broken insulation or when arcing takes place. Based on identification of power line noise, Mastenbrook (2001) describes a method to "hunt" for sources of stray RF emissions. The approach relies on a commercial air band amplitude modulation receiver and a dipole antenna system. The hardware described was used when RF power line noise had already been observed and specific poles and capacitor banks were to be identified as contributing to RF noise. When such electric circuitry carries high-frequency switching signals,

electromagnetic radiation is lost to the air as a by-product of designed operation. Often, this radiation can be identified more easily than can direct monitoring of power line 50/60 Hz field effects as this attenuation can be less severe with distance.

Vignati and Giuliani (1997) list recorded values of magnetic flux densities near transmission lines. Table 2 shows characteristic RF magnetic field intensities near transmission lines. In addition to the data in Table 1, Vignati and Giuliani (1997) reported a series of 207 kHz magnetic induction measurements with varying distances near 50 Hz commercial power lines. Figure 8 shows the data plotted and curve-fitted.

The induction intensity can be seen to decay monotonically with distance from the energized line. Figure 8 and Table 2 show that flux densities at a given distance are more substantial for 50-Hz magnetic induction than for RF induction.

Extrapolation of the data shows that sensors capable of delineating power line emissions to one-hundredth of a pico-tesla (pT) are required to identify such effects at 30,000 ft. This is problematic because sensor devices capable of this level of sensitivity will be subject to ionospheric charge carrier effects. At extremely high altitudes, the possibility of detecting power line RF emissions and delineating them from stray RF fields becomes impossible. Recognition of patterns of interference from power system operation, as described in Mastenbrook (2001) would rely on positive identification of signals with less than 1 uT intensity.

Table 2. Flux density magnitudes near 50 Hz power lines (Vignati and Giuliani 1997).

Site	50-Hz Magnetic Induction, B (μT)	RF Magnetic Induction, B (pT)	Distance to the Line (m)
A. Italy	2.4	308 at 112 kHz	8
B. Italy	5	120 at 179 kHz	14
C. Italy	—	197 at 270 kHz	18
D. Italy	1.1	270 at 270 kHz	28
E. Italy	4	123 at 175 kHz	13
F. Italy	1.6	120 at 370 kHz	45
	1.6	105 at 136 kHz	45
G. Sweden	—	200 at 330 kHz	18
H. Italy	0.8	438 at 136 kHz	19
	0.8	155 at 291 kHz	19
	0.8	97 at 370 kHz	19
K. Italy	1	116 at 150 kHz	18
	1	32 at 243 kHz	18

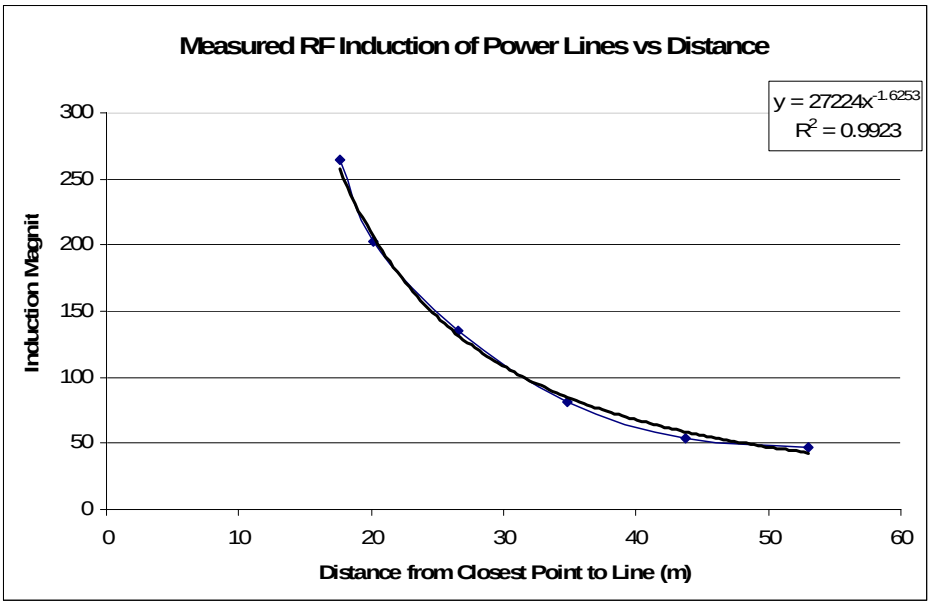

Figure 8. Measured RF induction near 50 Hz power lines (Vignati and Giuliani 1997).

No current technology has demonstrated the combination of power electronics architecture to operate at this low input signal strength when coupled with sensing mechanisms capable of detecting such minute emissions at near real-time speeds (Chapter 3 of this report discusses data management during surveillance in greater detail). In physical terms, the RF induction roughly varies with r^{-2} while 50 Hz magnetic induction (Eq 4) decays by r^{-1}. The difference between these attenuation levels becomes appreciable with large values of r.

Corona Effects

When an electrical conductor is charged to a sufficiently large voltage, the associated E field may become large enough to cause local ionization of the air at the surface of the conductor. Partial discharge is the result, as a consequence of ambient atmospheric ions that exist from photoionization, field emission or background radiation. In non-uniform fields (e.g., near a point) this local electric field may exceed a critical threshold field strength, E_c, at which point the electron concentration develops an avalanche nature, which is the precursor to dielectric breakdown (discharge) or corona onset (Kuffel and Zaengl 1984). These coronas may be either transient or steady state in nature and exhibit dependence on the weather conditions. Conductor moisture and surface irregularities can be the cause of local spikes in electrical field intensities and thus higher ionization losses. At 330 kV, power losses due to corona is typically on the order of 4 kWper three phase kilometer of transmission (Moore et al. 2005).

The critical field strength, E_c, has been determined for the special case of a coaxial cylindrical geometry in air. An empirical relation based on many measurements of E_c, different radii, r, of the inner conductor and atmospheric conditions has resulted in an expression of the form:

$$\frac{E_c}{\delta}(\text{kilo}-\text{volts}/\text{cm}) = \left(31.53 + \frac{9.63}{\sqrt{(r\delta)}}\right) F(r\delta) \qquad \textbf{Eq 5}$$

where:

$F(r\delta)$ is a dimensionless correction factor given by the piecewise function

$F(r\delta) = 1.0$, for $r\delta < 0.5$ cm,

$F(r\delta) = 1.0 - \left(.0234 \ln\left(r\delta\right) + .0262\right)$ for $0.5 < r\delta < 100$ cm

Here,

$$\delta = \frac{P}{76.0\text{cm}}\left(\frac{293^{o}\text{K}}{T}\right),$$

which is a dimensionless factor required to account for atmospheric pressure changes, where:

P is pressure in centimeters of mercury
the temperature T is expressed in degrees Kelvin
r in Eqs 5 and 6 is expressed in centimeters.

There is a distinct difference in the visual appearance of coronas, observed along wires of different polarity in applied voltage. Under positive voltage, corona appears in the form of a uniform bluish-white sheath over the entire wire surface. Experiments reveal the following sequence of events, along a linear conductor. As the surface electric field approaches that of E_c, the field distribution becomes increasingly less homogeneous; upon further voltage increase, a transient slightly branched filamentary discharge appears. These discharges have been shown to be identical to those observed under impulse voltages and are known as streamers. Under constant voltages the streamers appear and evolve with varying frequencies, giving rise to currents that are proportional to their physical length and are sometimes known as onset streamers or burst pulses.

When the voltage is increased further, the streamers become more frequent, until the transient activity stops, the discharge becomes self-sustained and a steady glow appears close to the positive surface. The glow gives rise to a continuous but fluctuating current, and further increase in voltage increases the luminosity of the glow, both in area and intensity. This particular corona glow develops only in the pres-

ence of negative ions, and any further increase in voltage gives rise to new and more energetic streamers. Ultimately, this leads to complete breakdown of the path between conductor and ground.

For the case of negatively charged wires, the corona appears differently, as reddish glowing spots distributed along the wire and the number of spots increases with the current. Again, experiments reveal the following sequence of events along a linear conductor charged near the critical electric field. With negative polarity and under static voltage conditions (near E_c), the current is seen to flow in very regular pulses, both in amplitude and duration. These pulses are known as "Trichel pulses," after their discoverer. The onset voltage is practically independent of gap separation (to ground), and in value is close to the onset of streamers under positive voltage for the same conditions.

The Trichel pulse mode can exist over a wide range of voltages and gap separations. Generally the frequency increases with voltage, depends upon conductor radius, gap separation, and pressure, with the pulse frequency observed to decrease with pressure. Eventually at much higher voltages, a steady glow discharge is observed, but this transition from pulse to glow discharge is not sharply defined (Kuffel and Zaengl 1984). Upon further voltage increase, the glow discharge persists until breakdown occurs. Breakdown under negative polarity occurs at considerably higher voltage than under positive voltage, except at low pressures. Probability of corona activity can be relatively high in older distribution infrastructure operating near amperage and voltage capacity. Hence under alternating power frequency voltage, the breakdown of non-uniform field gap invariably takes place during the positive half-cycle of the wave. This feature of the discharge necessitates the need for fast data capturing. If each half-cycle of the AC waveform cannot be discretized, corona may not be identified. Identifying corona is challenging since the ability to observe high-frequency corona requires fast optical instrumentation. Further, stroboscopic studies show that, with alternating (current) voltages, these corona features have about the same appearance as with constant voltage of the appropriate sign.

Corona Detection Methods

Dielectric breakdown of a material can be observed when an electric potential exceeds the dielectric strength of the material, such as air. Negative and positive charge carriers are pulled away from each other and the air molecules become ionized in the high electric field. A "cloud" of ions, or corona, forms and the air behavior changes from an insulator to a conductor. In such cases, measurable discharging currents can occur in air near conductors during dielectric breakdown. For air, the

breakdown field strength is on the order of 30 kV/cm. Typically, corona discharge is undesirable because of the associated charge losses during conduction.

Monitoring AC and DC corona can be a very informative method to identify and assess in-theater power systems. Moore et al. (2005) describe the concept of remote sensing and assessment of high voltage, by means of corona analyses and present the initial stages of the development of a novel voltage measurement technique that does not require contact with the point of measurement. This method involves the detection of the corona discharge induced at the point of measurement, as a result of the intense (local) electric field gradient. A particular feature of corona discharges is that they occur at a lower magnitude for negative voltages than for positive voltages. This is because the secondary processes that occur at the cathode for negative corona are delayed for positive corona, as the cathode is isolated from the ionization region by the drift region. The intensity of the radiation emitted by the discharge is also related to the polarity and magnitude of the applied voltage so the voltage can be measured.

Goetz et al. (1985) did laboratory tests to capture corona images at different negative and positive DC voltages, up to a maximum of 30 kV; the resulting images were processed to provide data for the training of neural networks (NNs) to recognize the different polarities and magnitudes of the applied voltages. They also presented some typical results from the initial tests. Related tests considered the UV light emitted from corona discharges. They presented the results of these initial tests to determine the feasibility of performing voltage measurement by UV detection. They also produced a spectral curve showing the intensity of the detectable radiation in both the visible and UV range.

The measurement of AC voltages is of greater significance when considering power system applications. Therefore, in the future stages of development of this technique, the method will be applied to AC corona. As this type of corona will be constantly changing, it will be necessary to incorporate high speed imaging procedures into the laboratory measuring system. Arrangements are being made to enable laboratory tests to be carried out with AC voltages up to 50 kV. The result of using such voltage will be a partial electrical discharge as a consequence of ambient ions accelerated by the field to energies capable of causing optical and sonic emissions in the adjacent air (discussed in more detail in the following section).

These discharges, which may be transient or steady state in nature, are known as "coronas," and can be remotely sensed given appropriate geometry and background conditions. A rough order of magnitude measure of this critical voltage may be found from the breakdown voltage of air, which is of order 30 kV per centimeter, at standard temperature and pressure (STP). Certainly, from a nearby vicinity, it is

quite unlikely that corona activity can be reliably identified with current state-of-the-art methods. Clearly, beyond addressing the DC corona limitation, a number of breakthroughs will be needed to incorporate corona analysis in remote assessment of power distribution networks.

Overview of Power System Remote Sensing Using Optical Assessment of Corona

Corona discharge near high tension lines indicates an energized system and can be used to estimate system reliability. Goetz et al. (1985) present a technique to optically and remotely monitor and measure corona. The approach is highly accurate and relies on capturing clear corona images near conductors at the millimeter level. According to the work, "intensity of radiation emitted by the discharge is related to the polarity and magnitude of the applied voltage." The work presents pixel intensities that relate corona discharge to system voltage levels.

Goetz's work is currently limited by many factors. "The current technique is limited to measuring DC voltages up to 30 kV at an accuracy of around 3–4%." AC corona cannot be monitored with the method outlined in their work as this would require fast, higher resolution optical capturing capability. Goetz indicates that "to be able to discern all the expected corresponding variations in emitted light, high speed imaging equipment will be required. This will enable the capture of several images for every half cycle of the AC voltage." For U.S. distribution, this equates to a capturing frequency of more that 200 Hz. Due to the 30 kV DC corona discharge limitation, the current approach is insufficient to monitor commercial power line activity until advances have been made in the monitoring of higher power signals.

Optical Determinations of Thermal Expansion and Line Sag

One of the direct consequences of electrical current flow through a conductor is ohmic heating and increase in temperature of the energized conductor. For all common materials this rise in temperature is accompanied by a corresponding change in physical size (thermal expansion). A measure of this change is embodied in the "Thermal Expansion Coefficient," α. The thermal expansion coefficient is defined to be the fractional change in material length, l, per unit change in temperature; thus: $\alpha = \Delta l/l$ (cm / cm-Centigrade). For many common structural conductors (Fe, Cu, or Al) this number is of order [11 to 24] x 10^{-6} (cm / cm-Centigrade), respectively. Thus if a conductor has a given length of l_0 (cm) at some initial temperature T_0 (C), then the expanded length, l(T) at a different temperature, T, is:

$$\ell(T) = \ell_0\left(1 + \alpha\left(T - T_0\right)\right) \qquad \text{Eq 6}$$

where:

T is degrees Centigrade
Eq 7 is expressed in centimeters.

Use of Eq (7) and knowledge of prevailing thermal environments is crucial in the design and layout of a power distribution system. Power lines are strung so as to provide maximal cable-to-ground clearance, for the largest conceivable cable temperatures that could result from ohmic and environmental heating. Conversely, sufficient cable length must be afforded between support towers so as to ensure that the cables are not over tensioned from episodic mechanical loading events, or very low operating temperatures of the power grid. One can make a crude judgment as to the relative activity of a power line system, by measuring the relative sag in the line for (known) physical cable properties, environmental conditions and prevailing power engineering practice. The sag can then be optically detected. Figure 9 shows the optical rate of advancement of commercial, civilian satellite systems.

Figure 10 shows the catenary geometry of a power line with uniform mass per unit length when suspended between two supports. This geometry is given by:

$$Y_c(X_c) = H\cosh\left(\frac{X_c}{H}\right) \qquad \text{Eq 7}$$

where:

Y_c is the height of the cable above ground
H is the height above ground of the lowest point of the cable's arc (10 m for the given example in Figure 10)
X_c is the horizontal span from the reference support point along the cable's arc.

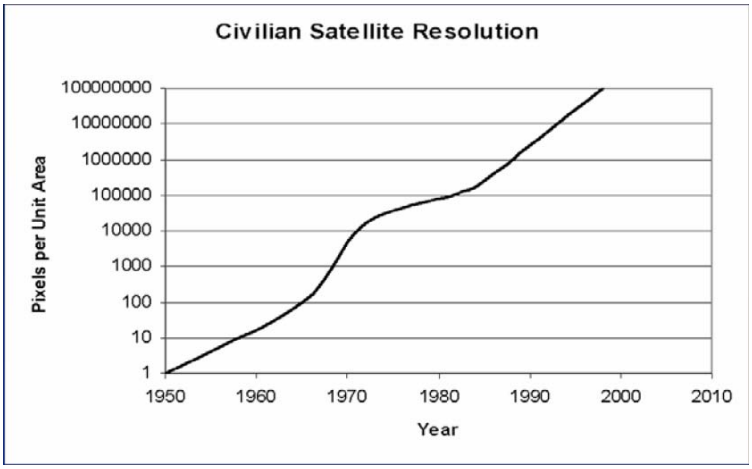

Figure 9. Recent civilian satellite systems exhibit orders-of-magnitude higher resolution than their predecessors in past decades.

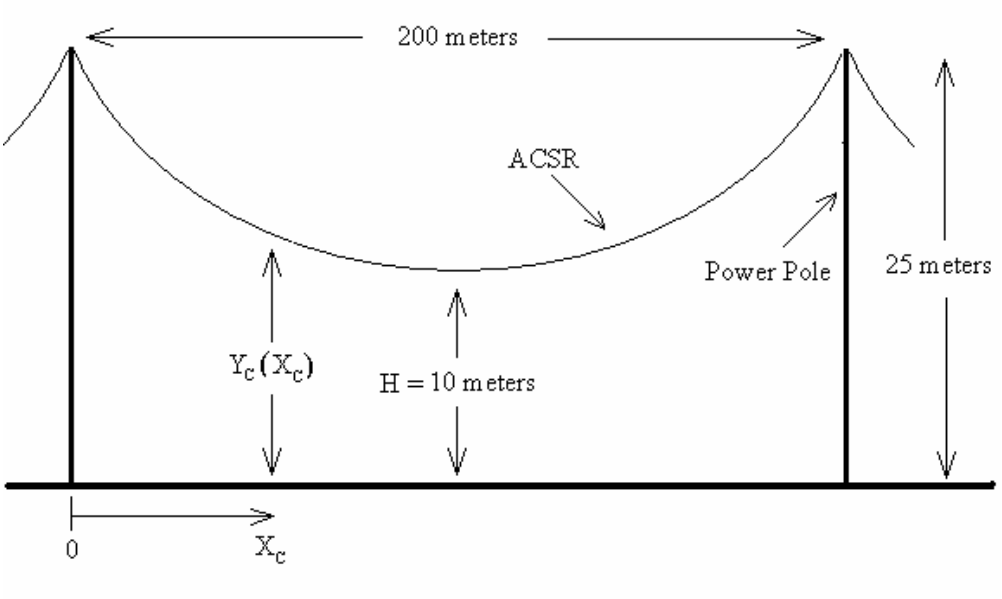

Figure 10. The catenary geometry of a power line.

When conducting high current, the cable will expand such that, at any instant, it will conform to the geometry given in Equation 8 with the additional arc length governed by Equation 7.

Because of high-resolution optical instruments, determining cable sagging can be far more manageable from great distances than direct identification of line temperature or electromagnetic emissions. Line temperature can be known if the sagging coefficient, ambient temperature, and catenary geometry can be observed. Because line spacing protocols, conductor type, and ambient temperature will vary in different regions, these dependencies can be removed by conducting analyses of several catenary geometries in a given region; energized (loaded) lines may be delineated from de-energized lines by observed additional sag (Figure 11). Multiple observations of the same caternaries can give insight to line loading patterns (critical lines in the infrastructure or lightly loaded sections).

By far, the most common conductor arrangement is the aluminum conductor steel reinforced line (ACSR). A typical Drake-type conductor will have a 900 ampere rating and a thermal coefficient at 75 °C of 0.125 ft/°C. Beyond 100 °C, however, because the expansion coefficient of aluminum is twice that of steel, most of the stress will be transferred to the steel core as the conductor's temperature rises. Eventually the core bears all the stress in the conductor. From this point on, the conductor as a whole essentially takes on the expansion coefficient of the steel core.

For a typical ACSR cable (Figure 12) at 54/7 (54 aluminum strands, 7 steel, 1-in. thick) this threshold point occurs around 100 °C (Dib 1999). A highly loaded line will sag an additional 2 ft for a 20 °C temperature increase in the line. For this case, an extremely loaded line during summer may sag nearly 2 m (cf. Eq. 7).

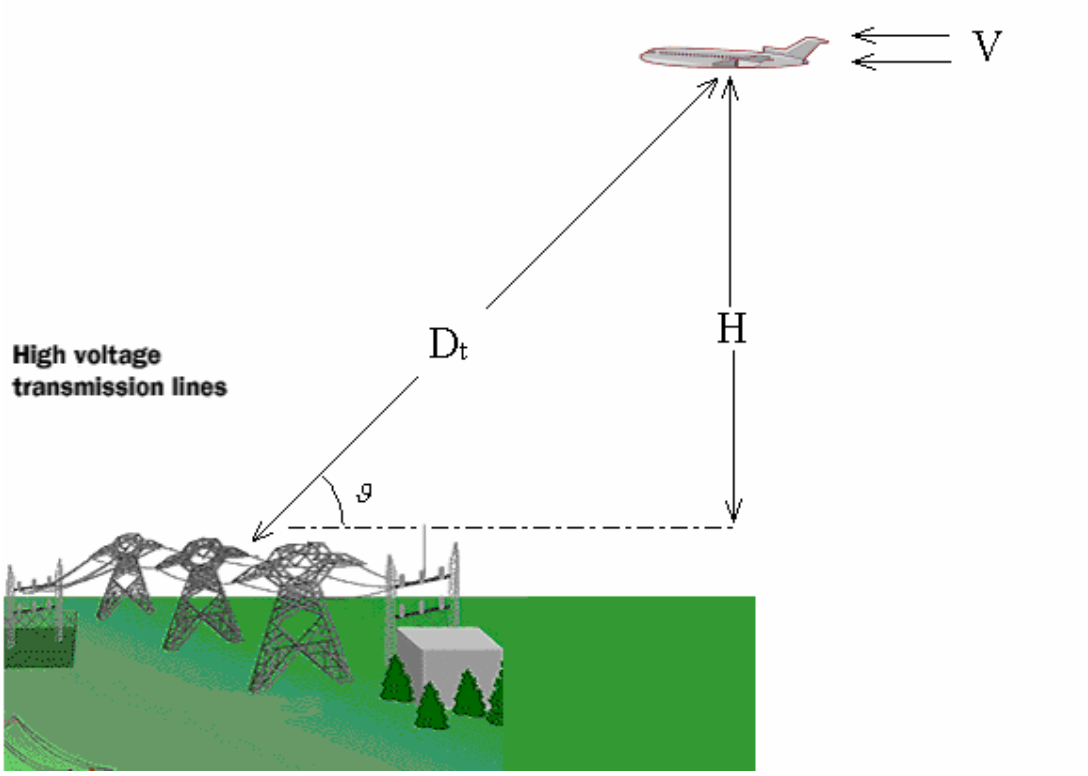

Figure 11. A surveillance craft monitors a sagging power line.

Optical Requirements and Target Distance Determinations

Consider the aerial UAV at "H" ft traveling at "V" mph (cf. Figure 11). One may begin to determine the "window of opportunity" available to capture line sagging in-theater by stating:

$$D_t = \frac{F}{RF} \qquad \textbf{Eq 8}$$

where:

F is the camera focal length
D_t is the distance to the target
RF is the representative fraction of the target.

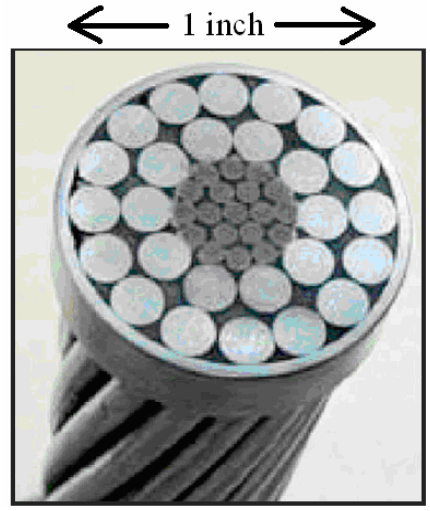

Figure 12. The cross-section of a power line; conducting aluminum members surround a supporting steel core (ORNL 2003).

Further, assume a monitoring instrument with an optical capability of M pixels in each dimension at a focal length of F_L mm. The distance D_t along any point in the flight path can be expressed as:

$$\frac{H}{\sin(\vartheta)}$$

where ϑ is the angle dividing the horizontal and the line adjoining the camera and target. A definition of the representative fraction is given by:

$$RF = \frac{X_{Image}}{X_{Target}} \quad \textbf{Eq 9}$$

where X_{Target} is the size of the target in one dimension and X_{Image} is the size the target occupies on the image in that dimension. The time available for monitoring is given by:

$$T_m = \frac{H(\tan\vartheta_1 - \tan\vartheta_2)}{V} \quad \textbf{Eq 10}$$

where ϑ_1 and ϑ_2 are the angles dividing the horizontal and the lines adjoining the camera and target at the beginning and end of monitoring, respectively. Using Equations 8 and 9, it can be shown that:

$$P_{Image} = \frac{F_L X_{Target} M \sin\vartheta}{H} \quad \textbf{Eq 11}$$

where P_{Image} is the number of pixels occupied by the target in one dimension.

Consider a monitoring craft traveling at 200 mph at 30,000 ft with a focal length of 300 mm with an optical window of 4000 pixels in each of the x and y dimensions (16 mega-pixel). The target is a line with a diameter of roughly 1 in. sagging 6 ft (determined in the previous section). Further assume that terrain features constrain monitoring between 450 °C < ϑ < 135 °C. The "window of opportunity" ™, given by Eq 10, is approximately 204 seconds. At ϑ=45 °C, Eq 9 predicts that the line will appear to be approximately 2.5 pixels thick and sag an additional span of 170 pixels. At ϑ=90 °C, the line occupies 3 pixels and the additional sag is computed to span 240 pixels. This means that a line sagging an additional 6 ft due to loading under the stated conditions will appear to be 170 pixels lower (when monitoring begins) and 240 pixels lower (when the craft is directly above the line).

Equation 12 can be used to predict the size of two-dimensional features when the dimensions of the target are known. In this instance, we can state that:

$$A_{Image} = \frac{F_L X_{Target} Y_{Target} M_x M_y \sin\vartheta}{H} \qquad \textbf{Eq 12}$$

where:

"X_{Target}" is the dimension of the target in one dimension as seen from aerial imagery
"Y_{Target}" is the other dimension of the target as viewed from aerial imagery
"M_x" is the optical resolution of the image in the dimension of "X_{Target}"
"M_y" is the optical resolution of the image in the dimension of "Y_{Target}"
"A_{Image}" is the number of total pixels occupied by the target footprint.

Note that increasing "F_L" can compensate for a higher flight path in Eqs. 10 and 11. This comes at the expense of compromised image quality as high values of "F_L" and "V" can result in blurred effects or a decreased depth of field, especially during low light operation.

Infra-Red Radiation

Infra-red radiation is a natural component of the electromagnetic spectrum, and is commonly perceived as heat radiating from warm bodies (FLIR Systems 2005). Near room temperatures (300 °K), this encompasses electromagnetic wavelengths between roughly 3 um to 8.6 um, which corresponds to a maximum peak in the blackbody spectrum, for this temperature. Since this radiation is adjacent to the visible spectrum, the capability to monitor and measure its properties has existed for a number of years. However the ability to extract useful information concerning thermal properties of a radiating material depends on a number of features, such the inherent emissivity of the material, thermal environment, relative distance and angular field of view subtended at the point of observation.

Some measure of the importance these factors produce can be found in the ideal blackbody radiation law: $S = \varepsilon\sigma T^4$. Here S is the total power flux (Watts per unit area) emitted by an ideal blackbody cavity, T is the absolute temperature in degrees Kelvin, and εσ are a set of radiative constants. In particular, σ is Stefan Boltzmann's constant which is $1.38*10^{23}$ $m^2s^{-2}K^{-1}$ and ε is the (dimensionless) emissivity of a given material, and depends entirely on the nature, geometry, and temperature of the emitting surface relative to the ambient environment. For an ideal blackbody cavity, $\varepsilon = 1$, independent of surface composition, and all real non ideal cavity surfaces have $0 < \varepsilon < 1$.

When little radiation input exists, an energized power line may appear to as a warm, linear feature. Extracting energization level of an identified line will depend on the density of thermal emissions per unit length along the system; this has a dependence on multiple system and non-system parameters (e.g., ambient temperature, solar insolation, transient operation, ohmic loss, etc). Therefore, remote assessments of the activity status of a power line based exclusively on its infra-red signature can be problematic at best. Reliably estimating the contribution of resistive heating in a power line to the overall thermal response signature would require solving a sparsely posed heat transfer problem. Such a problem requires more detailed information concerning solar radiance, time of day, ambient air temperature, wind speed and conductor surface properties for a proper resolution; Johnson et al. (1992) gives some background information. To overcome such difficulties, when multiple scans in a given theater can be performed, one can comparatively determine more intense signatures originating from energized infrastructure.

Hyper-Spectral Imaging

A technique called hyper-spectral imagery can identify and recognize power lines and power poles. Objects absorb, emanate, or reflect radiation (Figure 13) as a function of their constituent material. By using solar energy that has been reflected, sensors can capture material-unique target information (spectra). Image data is represented in layers captured over several wavelength bands. Features on the Earth's surface are captured in spectral absorption frequency windows (Figure 14).

Data can be captured in layers at hundreds of vary narrow bands from visible, near-infrared, infrared, short-wave infrared, and thermal infrared. This data can be used to determine and identify constituent elements of construction and land features. Sensors that collect multi-channel, contiguous, narrow spectral band imagery spanning from the visible to the infrared portion of the electromagnetic spectrum are generally referred to as hyper-spectral sensors (Canadian Space Agency 2005). Ultra-spectral imaging shares this definition with the exception that the

bands are extremely narrow; on the order of 1-2 nm in the visible and near-infrared. Multi-spectral imagery is typically tens of nanometers wide and are not necessarily contiguous. The power of the hyper-spectral sensor lies in its ability to record a fine spectral resolution electromagnetic profile for each pixel within its field of view.

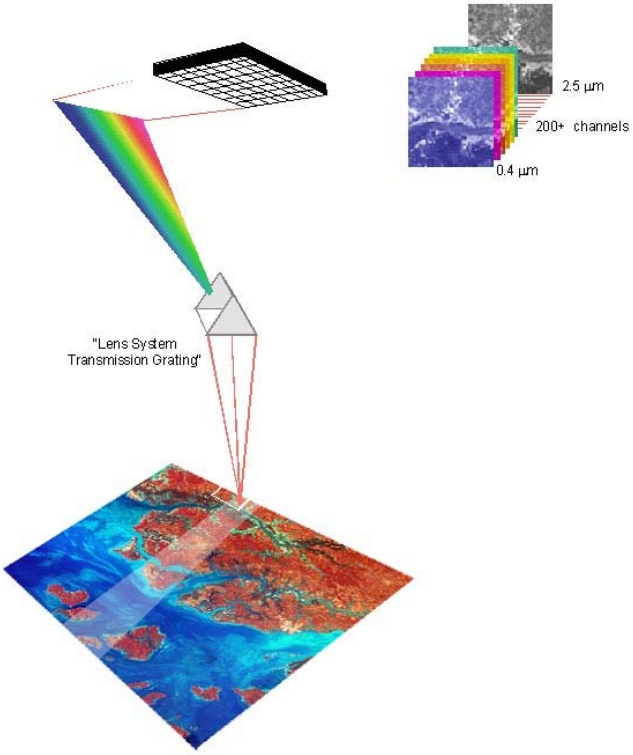

Figure 13. A hyper-spectral sensing system can measure feature radiation on the Earth's surface (Canadian Space Agency 2005).

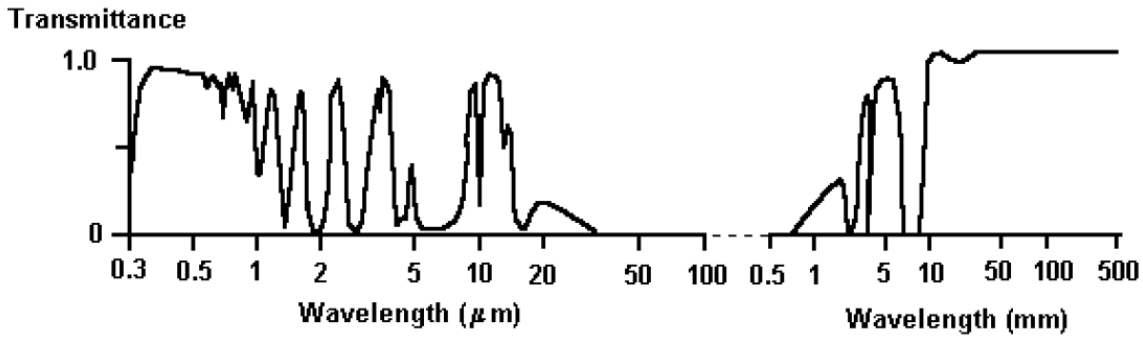

Figure 14. The wavelength "windows" generally used in remote sensing are defined by narrow spectral absorption bands.

Wavelength dependent characteristics in the reflectance or absorption spectra reveal important information about the chemical make-up and types of atomic and molecular bonding in the material being targeted (Goetz et al. 1985). Spectral features are the direct result of electronic and/or vibratory orbital energy transitions at the atomic and/or molecular level due to photon absorption. Thus the combination,

placement, and relative strength of the absorption feature(s) can be exploited for surface material identification, evaluation, and analysis of internal processes. The modular Imaging Spectrometer Instrument (MISI) is a line-scanning type hyper-spectral sensor with 72 channels from 0.4 µm to 1.018 µm (visible light ranges from about 0.4 µm to 0.7 µm) with 10 nm bandwidth each.

The MISI also includes 5 multi-spectral channels in the long-wave infrared (8-14 µm (2), 8-10 µm, 10^{-12} µm, and 12-14 µm) and 2 broad-band visible wavelength channels. The airborne visible/infrared imaging spectrometer (AVIRIS) operated by JPL is another good example of a hyper-spectral imager with 224 spectral bands, each with a 10 nm bandwidth, and covering the spectral range of 0.4 to 2.4 µm. Ustin's (2004) results suggest that a great deal of useful information can be obtained from hyper-spectral imagery, but the technique requires extensive off-line computer analysis. Some packaged software exists, but to maximize the usefulness of the remote data requires both ground truthing (hands-on field work), and a great deal of experience with both data analyses and a detailed knowledge of the remotely sensed object's physical parameters ("a Post-Doc, in every box"). Further, different targets require different analysis techniques, and the most productive techniques are often the result of empirical trials.

3 Aerial Surveillance Platforms and Data Management Capability

Unmanned Aerial Vehicles

Unmanned aerial vehicles (UAV) are commonly used to survey broad regions and terrains by flying above host nations. UAV altitude varies from a few hundred to 75,000 ft and hardware sophistication ranges from simple short-range mechanisms to advanced, self-reliant, intelligent, technically complex instruments. Typical UAV designs include extremely long wingspans, light weight materials, and extensive terrain-monitoring mechanisms. The UAV payload can consist of a number of independent systems to handle specific operations. Examples are IR communications, jammers, chemical/biological detection, laser designators and illuminators, and spectral sensors. UAVs can be equipped with an array of technologies to suit their purpose, clearly demonstrating the relevance of UAVs to remote sensing.

The Class IV UAVs are a pair of proposed FCS platforms supporting the unit of action (UA) commander. The Class IVa will be organic to the UA and provide wideband (WCP) long endurance time communications relay across the depth of the UA commander's combat radius. The Class IVb will likely be organic to the unit of employment (UE) and will provide wideband (WCP) relay to support network connectivity across the UA commander's area of influence.

To detect emission from infrastructure on the ground, sensing hardware, power and logic electronics, and data storage systems may be mounted in UAVs in the Class IV flight path. This will provide the opportunity for sensing mechanisms and systems to be "nearby" potential targets for the longest time duration. If we consider the example of optically monitoring commercial power lines (Chapter 2), maximum allowable UAV flight paths can be defined by requiring targets to occupy a given portion of an aerial image.

Data Acquisition and Processing

The field monitoring and data acquisition processes involved in the techniques reviewed earlier in this report can be as challenging as developing and implementing

the physical approach to assess infrastructure. These challenges can be classified as: (1) data transfer and processing, (2) lowering signal/noise ratios, and (3) geo-referencing.

Many difficulties can be attributed to physical limitations of data transfer, recording, and processing when large regions are monitored and discretized at high resolution. The data processing requirement of many hyper-spectral approaches can become prohibitive both in data acquisition and real-time processing. For example, many of the hyper-spectral approaches rely on recording multiple material-dependent properties (capturing more data than a typical aerial photo) over the discretized target region (e.g., reflectivity, absorbability, etc). This can amplify the data management challenge as multiple properties are required for each pixel, or picture element, to accurately define the electromagnetic profile of objects. Hyper-spectral approaches "produce vast quantities of data because of the number of bands simultaneously imaged" (Canadian Space Agency 2005). Bandwidth limitations alone can become a substantial bottleneck.

Consider the example given in the previous chapter to monitor a target region at 16 mega-pixel optical resolution at 10 fps over a 204 second duration, when tracking just a few data sets for each pixel requires a bandwidth exceeding 100 GB/s. For comparison, this is on the order of the fastest commercial graphics processors available today. The capability of monitoring instrumentation to detect low-amplitude, short-duration radiation to recognize patterns and signatures of active switchgear and other power system operations is also a current limitation. Sensor sensitivity and digital/analog filter limitations serve as bottlenecks to conducting on-the-fly signature detection.

The limitations described above are related to current technology and data processing barriers. As the state-of-the-art progresses and the amount of throughput at the logic design and analog electronics component levels increases, large target regions at high resolution can be captured, discretized, processed, evaluated, and compared to pre-defined signatures and radiation patterns for power system detection purposes.

A number of challenges in practical implementation and adoption of physical concepts to power system remote assessment exhibit no dependence on current commercial processing and bandwidth capabilities. For example, while future electromagnetic sensors may advance to have faster response times and lower power requirements, signal level attenuation will always be dictated by environmental parameters and geometry. For example, in the previous chapter, it was shown that the static electric and magnetic fields of a long, energized conductor decay with the distance from the target to the field point. At remote distances, the ambient field

due to that conductor exhibits a fixed attenuation level regardless of how advanced the sensor is.

One way to improve spatial resolution and also detect low strength signals is to place the sensor in closer proximity to the target. This in turn introduces a new set of challenges including survivability of the sensor platform and resolution of optical distortion (parallax).

4 Commercial Systems

The applications and commercial hardware described in this chapter are based on the first principles and physical phenomenon described earlier in this report.

Imager Inspection System

The Imager Inspection System (IIS) is a comprehensive state of the art remote detection and metering tool specifically designed to help assess and manage electrical grid infrastructure (Figure 15).* Because faults and service failures can be prohibitively costly, the IIS has been designed to locate potential system faults preceding outages. The system offers "the first comprehensive inspection of power transmission and distribution lines." Table 3 lists the IIS specifications.

Figure 15. Photograph of the Imager Inspection System.

* The IIS is a product of Aerospect Precision Imaging, a unit of the Utah State University Research Foundation, 1770 N. Research Parkway, Suite 195, North Logan, UT 84321; tel.: (435) 797-7420, accessible through URL: http://www.aerospect.com/homefla.html

Table 3. Specifications of the Imager Inspection System.

Sensors	Processing
Medium Field of Vision (FOV) Uses: structure and substation imagery Field of view: 23 – 215 ft (7 – 65 m) Resolution: 4H – 3.3H (0.93 – 10.3 cm) per pixel Wavelength: 350 – 700 nm.	***Automatic Detection Capabilities*** Structural defects IR hot spots Missing / broken insulators Change detection Corona hot spot Structure position location Point clearance
Wide FOV Uses: corridor imagery Field of view: 24 ft H x 38 ft V to 206 ft H x 349 ft V Resolution: 0.9H – 1.48H (1.19 – 10.9 cm) per pixel Wavelength: 350 – 700 nm.	***Optional Capabilities*** SF6 leak detection Wooden pole rot detection Vegetation classification and quantization
Narrow FOV Uses: component imagery Field of view: 8 – 125 ft (2.44 – 38.4 m) Resolution: 0.9H – 1.48H (0.24 – 3.77 cm) per pixel Wavelength: 350 – 700 nm.	***Mapping*** GPS location In-scene measurement
IR/Thermal Uses: thermal structure and substation imagery Field of view: 23 – 215 ft (7 – 65 m) Resolution: 0.4H – 3.3H (0.93 – 10.3 cm) per pixel Wavelength: 7.5 – 12 µm.	***Other System Options*** Ruggedized field computer systems Customer database integration Maintenance management software
Ultraviolet (UV)/Corona Uses: coronal structure and substation imagery Field of view: 23 – 215 ft (7 – 65 m) Resolution: 0.4H – 3.3H (0.93 – 10.3 cm) per pixel Wavelength: 7.5 – 12 µm.	***Software*** Grid Inspection Database System Online secure server 24/7 access Transmission Maintenance & Surveillance Interface User-friendly data viewer Windows™ based Desktop, laptop, or personal digital assistant (PDA) platforms Customer database integration
Laser Rangefinder ***Optional Sensors*** SF6 Leak Detection Wooden Pole Rot Detection Hyperspectral Imager (300 nm – 1000 nm)	

The IIS is aircraft-mounted and can provide "a high speed, precise, comprehensive, multi-spectral approach." The IIS can output high-resolution color imagery that includes geo-referenced indications of substation, tower, line, corona discharge, thermal imagery, and Electro Magnetic Interference (EMI) amplitude. By application of simple algorithms using corona and thermal patterns, IIS can distinguish between electrically hot and cold lines and substations. Additionally, the likelihood of future line faults can be assessed. Successful tests have been performed above 69 kV. Energized lines can be delineated from de-energized lines down to 69 kV at about 150 m. It has been determined that lower voltages are theoretically detectable, but have not been tested.

A given IIS fly-by path can orbit substations and gain detailed information regarding voltage levels of bus bars and thermal levels of substation transformers. Addi-

tionally, current and future faults can be identified by determining the level of corona discharge. Because the IIS features embedded GPS capability, the output of the IIS is a mapped, geo-referenced database with imagery and object properties. The on-board hardware includes 3–4 cu ft of detection equipment and a small computer (totaling 700 lbs) to be mounted on the craft exterior.

GEM-2A Introduction

One of the most well established physical phenomenon to detect or monitor metal objects is electromagnetic interference. Electric charges will flow in conductive objects when an electric potential is applied across them. Current can also be observed in such objects when placed in a magnetic field resulting from a nearby distribution of current. This consequential, or induced, current emanates a secondary magnetic field. Field sensors can identify this field and detect the presence of a conducting object. As explained later, advanced systems may identify frequency-dependent properties of target objects.

Won et al. (2003) show that the method outlined above is principally intended to detect the existence and location of an object emitting a secondary field. "Frequency sounding" is a more sophisticated approach to detect attributes such as the size, material, or location of the object by characterizing the secondary, consequential field. Phase shifts and amplitude attenuations shifts between the fields are indications of object attributes. Won et al. (2003) state:

> When an electrically conductive and/or magnetically permeable object (e.g., landmine, or ebody) is placed in a time-varying EM field, a system of induced current flows through the object. By observing a small secondary magnetic field emanating from the induced current, we attempt to detect the object; this is the foundation of the EMI method. If, in addition, we can measure a broadband spectrum of the secondary field, we may obtain a distinct spectral signature that may identify the object. Based on the response spectrum, we can "fingerprint" the object … which is the concept of EMIS. By using the EMIS responses from known or producing deposits as fingerprints, we look for locations having similar spectra within a local mineral province.

Description

The normal GEM system consists of a transmitter, bucking coil and receiving coil arrangement (Won et al. 2003). Its primary use is as a metal detector or geological exploration tool. The receiver is essentially a low frequency spectrum analyzer (effectively DC to 96 kHz). Operators normally discard data from everything except

their transmitted frequencies, but happened to plot the 60-Hz magnetic field amplitudes from a southern Michigan survey area in one of their reports using a helicopter-towed device (Figure 16). (Table 4 lists the specification of the GEM-2A.)

> The survey was flown east-west over an area of approximately 12 km by 18 km at an north-south line spacing of 320 m. Commensurate with population, the survey area has dense powerline grids along with at least two major north-south transmission lines at a height of about 50 m. Many smaller powerlines are 10–30 m high in this area. The survey helicopter, flying at a nominal altitude of 60 m (~200 ft), towed the bird at 30 m. (Won et al. 2003)

Figure 16. A photograph of the GEM-2A helicopter-towed sensing system (Won et al. 2003).

Table 4. Specifications of the GEM-2A helicopter-towed sensing system (Won et al. 2003).

Parameter	Specification
Total length and weight	643 cm (21.1 ft); 120 kg 9250 lb)
Tow cable length	35 m (120 ft); diameter 2,54 cm (1 in.)
TX-RX separation	510 cm (16.7 ft)
Coils configuration	Horizontal coplanar
Transmitter current	60 amp RMS max.
Transmitter moment	500 Am^2 at 330 Hz; 160 Am^2 at 1 kHz 16 Am^2 at 10 Hz; 4 Am^2 at 40 kHz
Power supply	28 VDC
Frequency range	300 Hz to 48 kHz
Number of frequencies	Programmable (typically 5)
Sampling rate	30 samples/sec for all used frequencies

The data used to generate the image of magnetic intensities in Figure 4 (p 9) is entirely passive. For powerline mapping, the same data could be taken with the

GEM-2, a hand carried surveying device. However, this instrument does not normally record this information and some modifications would have to be made to the device. Analysis would likely be done with a laptop computer attached to the device. Line loads could be analyzed by frequency spectrum fingerprinting (e.g., harmonic analysis). Other potential applications may include non-contact power metering. The GEM -2A weighs about 150 kg, but because it is primarily composed of an "active" EM system (transmitting and receiving coils), this detection approach is friendly to hardware miniaturization. The EM bandwidth, which is somewhat dependent on environmental noise, is generally from 270 Hz to 48 kHz.

"Passive" systems similar to the GEM system can operate with reduced hardware (which makes them less detectable), and offer the advantage of being more UAV-friendly. Such passive detection instrumentation can be accommodated in a much more compact form (perhaps 2 cu ft).

GEM-2A System Operation

Adjusting the broadband sensor to 50/60 Hz baseline frequency allows the user to passively view the EMI amplitude of the 50/60Hz harmonic. In this way, power line effects can be detected from within a few hundred feet. An alternate means to detect signatures of other power system components is to vary the base-line frequency. A "sampling" frequency is determined and, for a fixed frequency at or below the sampling rate, a discrete time-domain spectrum can be determined using the hard-wired forward Discrete Fourier Transform (DFT). The advantage of such an approach is that the unique signatures of distribution system members may be more easily discernable in the broadband spectrum at various frequency bands and, in addition, all these ranges can be accommodated with a single flight.

To display field-effect magnitude with respect to the X-Y plane, we can obtain geo-referenced output using the embedded GEM-2A GPS capability. One option is to spatially superimpose the output of the scanned region with optical/thermal/graphic representations of the same region. The existing GEM-2A hardware has been adequately tested and is in the commercial use stage. DARPA is employing the system for underground facility detection while another EM-mapping effort in the Yucca Mountains currently underway covers 12,000 line miles with an estimated cost of $70-80/mile. System operation cost is a determinant of the number of line miles; for example, a modest effort covering 500 line miles may cost $200/mile.

Switching Transient Fields in Substations

One of the most direct ways to identify energized systems is measuring field magnitudes near substations and substation bus bars. Many academic efforts have addressed estimation and prediction of the field in the substation switchyard under varying network topologies and substation constructions.

When a bus segment (20 –150 ft) inside above the switchyard is energizing and de-energizing, transient fields can be detected. Because fast switchgear can deliver pulses of high currents and voltages, up to several thousand EMI induced switching transients are detectable at air and gas insulated substations operating between 115 and 500 kV. The magnitude of field transients and bursts is quantified in a "macroburst":

> The totality of all transients (arcs) produced during a single switch operation is termed a macroburst. A macroburst can be characterized in terms of its duration in time, the total number of field transients produced, the amplitude variation between the smallest and largest transient, and the pulse repetition frequency (PRF). (Wiggins and Wright 1991)

Additional insights regarding the nature of switching can be inferred from the switching interval. Manual hand-operated disconnects (HOD) may occur over up to a 2-second interval (120 cycle) and may yield up to 10,000 small transients (Wiggins and Wright 1991). Motor operated disconnects (MOD) occur over a shorter duration and result in less transients. The individual transients are termed micropulses. "Each micropulse is the result of a single arc occurring across the gaps of a switch during opening or closing."

5 Conclusions

The site selection challenge in forward theaters remains a pressing technical and logistical difficulty for military planners. One candidate solution is to solve the region aggregation problem with discretized geographic, terrain, and infrastructure data models. The types of infrastructure data that can be considered are proximity to roads, railways, buildings, wireless transmitters, and electrical transmission and distribution networks. Because no military presence exists in a candidate region, assessment of infrastructure must be achievable using remote means.

This work has reviewed several advanced strategies to evaluate electrical system infrastructure using remote techniques. The methods vary in achievable resolution, susceptibility to noise and surroundings, maximum target distance, equipment size, and data requirements. Another practical factor by which the approaches can be delineated is whether or not a given strategy is likely to become more practical with technical advancements in data processing, signal pattern recognition, optical imagery, and circuit miniaturization.

This study concludes that the optical assessment methods (including hyperspectral sensing) outlined are by far the most effective ways to gather information about in-theater infrastructure from great distances (>> 500 ft). These techniques offer minimal signal attenuation and atmospheric undesirable interference (when monitoring is performed in the low attenuation bands shown in Figure 14). TEC (2005) shows current commercial and civil sensing platforms and their spectral and spatial specifications. The resolution of civilian satellite systems has improved nearly exponential since 1950 (Figure 9, p 18). This allows for detection of physical dimensions of infrastructure to within a few meters from space. It is difficult to conceive of sensor design in the near future that will allow for assessment at this level and accuracy using RF, acoustic, or thermal characterization. Equally challenging is the task of detecting the power level conducted over a region of transmission or distribution at great distances. Detecting the energized state and power level in a given corridor using RF emissions has been shown to be extremely unfeasible. Such network features are more easily detected using magnetic field emissions (50 Hz/60 Hz) based on Eq 4 (p 8).

This study recommends that future research include development of filters capable of assessing features gathered from thermal and electromagnetic detectors. For this to occur, patterns must be identified associating measured signal levels to voltage

and current values transmitted through power corridors. One potential approach would be to capture the electromagnetic profile of a target region (e.g., Figure 4, p 9) and then scan the same area using instrumentation similar to that shown in FLIR (2005). For a given system, more pronounced thermal signal (sometimes referred to as high contrast) levels may be correlated to higher power level transmission in the corridor. Upon a reasonably accurate solution to this challenge, electric utility transmission and distribution assets can be inferred when only incomplete schematics of the system are available.

Bibliography

Aerospect Precision Imaging (Utah State University 2003), accessed through URL:
http://www.usurf.org/units/aerospect

Canadian Space Agency, *Hyperspectral Remote Sensing* (Canadian Space Agency), accessed November 2005 through URL:
http://www.space.gc.ca/asc/eng/satellites/hyper_forestry.asp ????
http://www.space.gc.ca/asc/eng/csa_sectors/earth/hyper_military.asp

Dib, Ramzi, *Line Parameters of Overhead Power Lines and Their Calculation Using the EMTP/ATP Line Constants Program* (08 Oct 1999), accessed through URL:
http://www.ece.umn.edu/class/ee4721/line_constants_notes.pdf

Energy Network Assn., *Electric and Magnetic Fields* (National Grid plc), accessed Nov 2005 through URL:
http://www.emfs.info/Source_transmission.asp

FLIR Forward Looking Infra-Red (Infrared), accessed through URL:
http://www.x20.org/thermal/FLIR.htm

FLIR Systems, *Infrared Camera Success Stories* (FLIR Systems, Boston, MA, 2005), accessed through URL:
http://flirthermography.com/success

GEOPHEX Engineering, accessed November 2005 through URL:
http://www.geophex.com

Goetz, A.F.H., G. Vane, J.E. Solomon, B.N. Rock, "Imaging Spectrometry for Earth Remote Sensing," *Science*, vol. 228, No. 4704 (1985), pp 1147-1153.

Information Ventures, Inc., accessed (November 2005) through URL:
http://infoventures.com/private/federal/q&a/qaenvn2a.html

Johnson, Keith R., Allen R. Curran, and Teresa G. Gonda, *Present State and Future of Infrared Signature Models,* presented at the 3rd Annual Ground Target Modeling and Validation Conference Michigan Technological University (Houghton, MI, August 1992).

Kuffel, E., and W.S. Zaengl, *High Voltage Engineering* (Pergamon Press Inc, Elmsford, NY, 1984).

Mastenbrook, Gary, *Power Line Noise Hunting* (Schaumberg, IL, 12 April 2001), available through URL:
http://www.qsl.net/n8dmt/powerline.html

Moore, P.J., D.L. Hickery, and M.G.G. Urbaneja, *Remote Sensing of Voltage Using Optical Assessment of Corona* (Institute of Electrical and Electronics Engineers [IEEE], 2005), available by subscription to IEEE though URL:
http://scholar.google.com/url?sa=U&q=http://ieeexplore.ieee.org/iel5/6967/18765/00867543.pdf

National Nuclear Security Administration (NNSA), *Multispectral Thermal Imager (MTI)* (National Nuclear Security Administration, 08 June 2004a), accessed through URL: http://nis-www.lanl.gov/nis-projects/mti/

NNSA, *Multispectral Thermal Imager (MTI)* (National Nuclear Security Administration, 08 June 2004b), accessed through URL: http://www.fas.org/spp/military/program/masint/mti.htm

Outdoor Powerline Conductor Accelerated Testing (PCAT) Facility Now Operational, Oak Ridge National Laboratory (ORNL) Fact sheet ORNL 2003-01957/jcn (ORNL, Oak Ridge, TN, 2003), accessed November 2005 through URL: http://www.ornl.gov/sci/oetd/documents/03-01957_PCAT1.pdf

Topographic Engineering Center (TEC) Imagery Office (TIO), accessed November 2005 through URL: http://www.tec.army.mil/tio/

Questions and Answers About EMF Electric and Magnetic Fields Associated with the Use of Electrical Power (Information Ventures, Inc., January 1995), accessed through URL: http://infoventures.com/private/federal/q&a/qaenvn2a.html

Ustin, S., *Applications of Hyperspectral Imagery for Threatened and Endangered Species Habitat Determination at Military Installations* (UC Davis California Space Institute Center of Excellence and the Center for Spatial Technologies and Remote Sensing, ERDC-CERL, 11 February 2004).

Vignati, Maurizio, and Livio Giuliani, *Radiofrequency Exposure Near High-Voltage Lines*, *Environmental Health Perspectives* vol 105, Suppl. 6 (1997), pp 1569-1573, accessed November 2005 through URL: http://ehp.niehs.nih.gov/members/1997/Suppl-6/vignati-full.html

Wiggins, C.M., and S.E. Wright, "Switching Transient Fields in Substations," *IEEE Transactions on Power Delivery*, vol 6, No. 2 (IEEE, April 1991).

Won, I.J., Alex Oren, and Frank Funak,"GEM-2A: A Programmable Broadband Helicopter-towed Electromagnetic Sensor," *Geophysics*, vol. 68, No. 6 (November-December 2003), p 88–1895. http://www.tec.army.mil/tio/

Wallace, Robert M. "Constraining Shape in Region Aggregation Modeling," manuscript submitted to *International Journal of Geographical Information Systems*, November 2003.

Acronyms and Abbreviations

Term	Spellout
ACSR	aluminum conductor steel reinforced line
AIS	Air insulated substation
AVIRIS	airborne visible/infrared imaging spectrometer
CERL	Construction Engineering Research Laboratory
DARPA	Defense Advanced Research Projects Agency
DC	direct current
DFT	Discrete Fourier Transform
EM	enlisted men
EMI	Electro Magnetic Interference
EMIS	Electromagnetic Induction Spectroscopy
ERDC	Engineer Research and Development Center
FCS	Future combat system
F_L	Focal length
FOV	Field of View (FOV)
GB	Gigabyte
GPC	Ground control points
GPS	global positioning system
HOD	hand-operated disconnects
IEEE	Institute of Electrical and Electronics Engineers
IIS	Imager Inspection System
MISI	modular Imaging Spectrometer Instrument
MOD	Motor operated disconnects
PDA	personal digital assistant (PDA)
PO	purchase order
PRF	pulse repetition frequency
RDTE	Research, Development, Test, and Evaluation
RF	Radio Frequency
RFI	Radio Frequency Interference
RMS	Root-mean square
SI	System International
STP	Standard temperature and pressure (STP)
UA	unit of action
UAV	unmanned aerial vehicle
UE	Unit of employment
URL	Universal Resource Locator
UV	Ultraviolet
VDC	volt DC
WCP	wide band
WWW	World Wide Web

REPORT DOCUMENTATION PAGE

Form Approved
OMB No. 0704-0188

1. REPORT DATE (DD-MM-YYYY)	2. REPORT TYPE	3. DATES COVERED (From - To)
02-2006	Final	

4. TITLE AND SUBTITLE
Techniques To Remotely Identify and Evaluate Electrical Power System Infrastructure

5a. CONTRACT NUMBER

5b. GRANT NUMBER

5c. PROGRAM ELEMENT NUMBER

6. AUTHOR(S)
Tarek Abdallah, Michael K. McInerney, William R. Taylor, and Carl A. Feickert

5d. PROJECT NUMBER
622784AT41

5e. TASK NUMBER

5f. WORK UNIT NUMBER
8H08FB

7. PERFORMING ORGANIZATION NAME(S) AND ADDRESS(ES)
U.S. Army Engineer Research and Development Center (ERDC)
Construction Engineering Research Laboratory (CERL)
PO Box 9005
Champaign, IL 61826-9005

8. PERFORMING ORGANIZATION REPORT NUMBER
ERDC/CERL TR-06-2

9. SPONSORING / MONITORING AGENCY NAME(S) AND ADDRESS(ES)
Headquarters, U.S. Army Corps of Engineers (HQUSACE)
441 G. St., NW
Washington, DC 20314-1000

10. SPONSOR/MONITOR'S ACRONYM(S)
CEERD-CV-ZT

11. SPONSOR/MONITOR'S REPORT NUMBER(S)

12. DISTRIBUTION / AVAILABILITY STATEMENT
Approved for public release; distribution is unlimited.

13. SUPPLEMENTARY NOTES
Copies are available from the National Technical Information Service, 5285 Port Royal Road, Springfield, VA 22161.

14. ABSTRACT

It can be difficult for military planners to assessing potential sites when establishing forward facilities for deployed military units in austere environments. They must consider many parameters, e.g., geographic elevation and contiguous flat terrain, proximity to operating electrical distribution systems, etc. Since potential site locations may be in hostile territory, remote detection and assessment of electrical systems can be essential. Because such systems emit signals and/or have passive signatures, a potential source of identification can be examined when viewed from above the earth or from a distance when on the ground. This work reviewed the basic signal and signatures of electrical systems and identified parameters most pertinent to their remote detection

15. SUBJECT TERMS
remote sensing
electromagnetic emissions
electrical distribution system
electrical systems
military planning

16. SECURITY CLASSIFICATION OF:			17. LIMITATION OF ABSTRACT	18. NUMBER OF PAGES	19a. NAME OF RESPONSIBLE PERSON
a. REPORT	b. ABSTRACT	c. THIS PAGE			Tarek Abdallah
Unclassified	Unclassified	Unclassified	SAR	52	19b. TELEPHONE NUMBER (include area code) (217) 373-73754432